International Journal of Academic Engineering Research (IJAER)
ISSN: 2643-9085
Vol. 4, Issue 8, August – 2020, Pages: 6-9

Effect of Boron Content on Strain-Hardening Exponent in Recycled Steel

Christopher Senfuka[1], Paul Kizito[2]

[1] Dept of Mechanical Engineering, Kabale University
P. O .Box 317, Kabale

[1] senfukac@kab.ac.ug

[2] Dept of Mechanical and Prod. Engineering, Kyambogo University

[2] kizito.muburu@yahoo.com

Abstract— *While the elastic zone in the deformation process of materials is mainly represented by a linear function of gradient E, the plastic portion has been characterized by various exponential functions with an exponent n that varies with its chemical composition, the level of work hardening and the material in question among others. Recycled steel, whose composition depends on the source and availability of its raw material, has an extremely vulnerable n-value. In this paper, the effect of the boron content in recycled steel on the n-value of thermo-mechanically treated bars made from it has been studied. To do this, TMT bars were subjected to tensile testing and the corresponding force extension diagrams plotted. The values of* ε_{i10} *and* ε_{i20} *for the interval between 10% and 20% deformation respectively were determined to correspond to the stress values* σ_{i10} *and* σ_{i20} *so that* $n_{i(20-10)} = \frac{(ln\sigma_{i_{20}} - ln\sigma_{i_{10}})}{(ln\varepsilon_{i_{20}} - ln\varepsilon_{i_{10}})}$ *was calculated as the ruling n-value for each interval. Spectro-analysis was used to determine the chemical composition of the samples so that the percentage boron content by weight was plotted against the n-value. The growth of the n-value with boron content has been shown to obey a polynomial function and to enhance the tendency to strain-hardening, implying early onset of failure in pronounced cold deformation.*

Keywords: Boron content, cold working, hardening coefficient, strain hardening.

I. INTRODUCTION

The significance of plastic deformation in metals often makes its quantification a fundamental step in both the design of processing metal working tools and that of actual components. The natural starting point is the load-extension curve as the graphical representation of the relationship between the stress obtained by measuring the load applied on the specimen and the strain derived from evaluating the resulting deformation. This flow curve comprises an elastic portion obeying Hooke's law and a plastic portion featuring permanent deformation and follows the yield point of the curve The curve for many metals in the region of plastic deformation can be expressed by the Hollomon strain-hardening equation,

$$\sigma = K\varepsilon^n \dots\dots\dots\dots\dots\dots\dots\dots i)$$

where *n*, the n-value, is the strain-hardening exponent and *K* is the strength coefficient [1].

At the beginning of the yield phenomenon, plastic deformation prompts an out pour of dislocation movements along the slip planes. Further plastic deformation is curtailed by the interaction between the stress fields of the dislocations which impedes their motion through their mutual repulsion or attraction [2]. Additionally, when dislocations cross, they tend to entangle. These entanglements together with jogs and kinks act as pinning points which oppose dislocation motion, resisting deformation and subsequently leading to work-hardening depicted by increased yield strength,$\boldsymbol{\sigma_y}$. At any given time therefore, there is a correlation between the growth in yield strength and the dislocation density as given by equation *ii)* [3]:

$$\Delta\sigma_y = Gb\sqrt{\rho_\perp} \dots\dots\dots\dots\dots\dots\dots\dots ii)$$

where *G* is the shear modulus, *b* is the Burgers vector, and $\rho_\perp$ the dislocation density.

Further to this, the introduction of foreign atoms into a crystal in the form of alloying elements creates pinning points in the material. This is because these atoms are inherently point defects which create stress fields when placed into crystallographic positions and so block the passage of dislocations; resulting in solid solution strengthening [4]. Even if the alloying atom were the same size as the host material and did so not stress the lattice, it would have a different elastic modulus which would create different terrains for the moving dislocation and engender resistance to their movement [5].

The presence of solutes above a certain concentration also leads to the formation of second phase particles (precipitates) as a chemical combination between these solute atoms and other component element atoms present in the system such as iron in the case of steel [6]. These second phase particles cause lattice distortions which appear when the precipitate particles differ in size and

crystallographic structure from those of the host atoms [7]. The particles of the second phase precipitates act as pinning points just like solute particulates, impeding the movement of dislocations through the lattice and causing precipitation strengthening. The dislocations can cut through the second phase particles in the process of their movement or may bow around the particle as in Orowan strengthening [8]. This bowing results in the production of dislocation loops around the second phase particles leading to dense intertwining of dislocations and consequent hardening. The dislocation motion created by the deformation process experiences resistance around the second phase precipitates in much the same way as that of foreign atoms.

Strain-hardening is associated with increase in both the yield stress $\boldsymbol{\sigma_y}$ and the ultimate stress $\boldsymbol{\sigma_u}$ although the rate of increase of the former with deformation is higher than that of the later (Fig.1). This leads to the ratio σ_y/σ_u to tend to unity with growing deformation. This means that failure occurs closer to yield with growing deformation. This loss of ductility with the growing n-value is a natural result of the impeded dislocation motion and is in consonance with plastic deformation prior to fracture. This is appreciable in large angle bending frequently required in building construction practice (Fig.2).

It has been argued that Boron, an interstitial element in steel, takes on both solid solution and precipitation strengthening mechanisms under different circumstances to constitute the source of strain-hardening for steel of low carbon content [9].

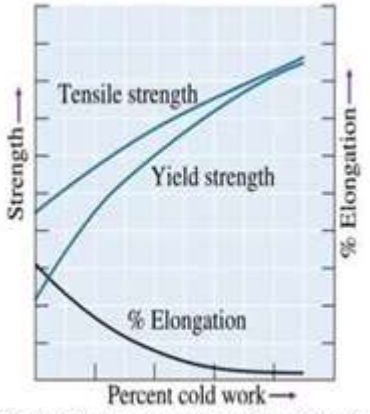

Fig. 1: Change properties with cold work

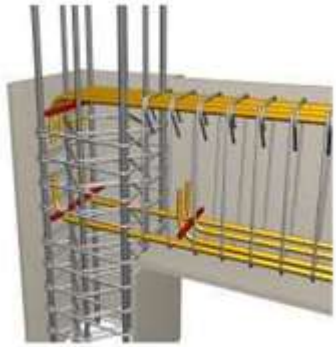
Fig.2: Large angle bends

The major source of boron in recycled steel is the induction furnace ramming mass refractory although much of it is also contributed by the scrap row material. Induction furnaces are preferably lined with 1.3 to 1.4 % boric acid sintered monolytic refractory fire bricks. This is done to enable them to withstand sudden thermo-shocks, temperature gradients of the order of 300-400°C for each centimeter of thickness across the lining and substantial electro-dynamic and chemical effects of the molten metal [10].

The boric acid (H_3BO_3) in the alumina and silica refractory, when exposed to heat, forms boron trioxide, B_2O_3 which is then reduced to boron by carbon at high temperatures. The boron is subsequently dissolved in the liquid iron [11]. It is this boron which is free of oxygen and nitrogen that precipitates as a complex carbide $Fe_{23}(C,B)_6$.

Considering the erratic nature of the tramp element distribution in recycled steel, large variations in boron content are naturally recorded and with them, unpredictable strength related phenomena such as strain-hardening.

The purpose of this research is to quantify the correlation between steel boron content and the strain hardening in low carbon recycled steel through the determination of the strain hardening index of different levels of boron content for commercially used thermomechanically treated bars.

II METHODS AND EQUIPMENT

Thirty thermo-mechanically treated reinforcement bars randomly selected from different outlets were subjected to tensile testing using the Testomatic Tensile Testing Machine. Since the n-values naturally vary with carbon content and the effect of boron depends on the level of carbon [12], the %C range for the thirty samples selected was controlled, being confined to 0.10 to 0.12% with a Cr content of less than to 0.30 % and the content of V not exceeding 0.05 for an average carbon equivalent of 0.5.

Taking into account that equation *i)* can be rewritten as $n = \frac{\varepsilon}{\sigma}\frac{d\sigma}{d\varepsilon}$, the strain rate was also regulated, being fixed at 0.13 mms^{-1} to eliminate the effect of the deformation rate, $d\sigma/d\varepsilon$ on the measured values. The rest of the parameters were set in accordance to US 155-2 [13]. The corresponding force extension diagrams were duly machine plotted.

International Journal of Academic Engineering Research (IJAER)
ISSN: 2643-9085
Vol. 4, Issue 8, August – 2020, Pages: 6-9

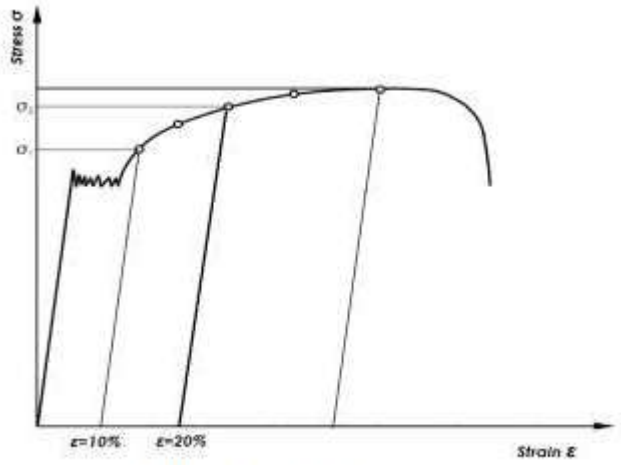

Fig.3: Stress-strain diagram

An initial value of stress at 10% was determined as in Fig.3. Another 10% deformation was then located on the diagram to reach 20% deformation and the corresponding stress value determined for each sample.

Using Hollomon's equation, $\sigma = K\varepsilon^n$, the value of $n_{i\ (20\text{-}10)}$ for $i = 1$ to $i = 30$ corresponding to the interval 10% and 20% deformation was determined for the logarithmic equation:

$$(ln\sigma_{i20} - ln\sigma_{i10}) = lnK + n_{i_{(20-10)}}(ln\varepsilon_{i20} - ln\varepsilon_{i10})$$

The value of the strain hardening index for the interval became:

$$n_{i(20-10)} = \frac{(ln\sigma_{i_{20}} - ln\sigma_{i_{10}})}{(ln\varepsilon_{i_{20}} - ln\varepsilon_{i_{10}})} \ldots\ldots\ldots\ldots\ldots\ldots\ldots\ldots iii)$$

The samples were subjected to spectro-analysis using a Spectro Arc Spectrometer.
A plot of the $n_{i(20\text{-}10)}$ against the corresponding boron content percentage was made in the Excel format and the curve of best fit made.

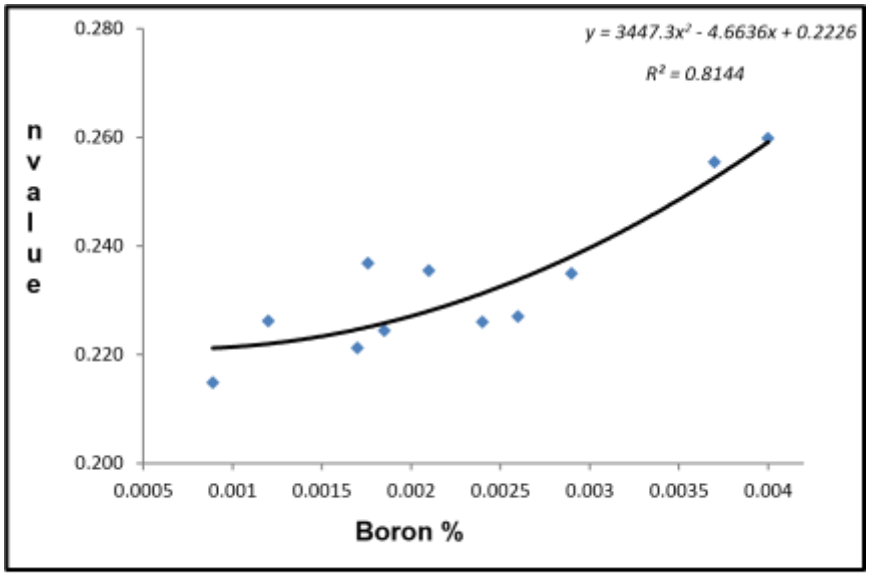

Fig.4: Variation of n-value with B content for TMT bars

III. RESULTS AND DISCUSSION

Fig.4 shows the plot for thermo-mechanically treated bars. A quadratic type equation makes the best fit with R^2=0.8.
The presence of boron in substantial amounts in the samples analyzed has led to increased susceptibility to work hardening. This tendency has been shown to increase quadratically with growing boron content.
The n-values obtained lay in the range 0.22 to 0.26 for boron content 0.0009 to 0.0037%. The large variation on the boron content and consequently, the n-values, shows the limited reliability of the steel for cold forming purposes, making it hard to select appropriate ingots for such operations.

In conclusion, the curve obtained in Fig.4 can be used to relate the boron in the steel chemical composition to specific level of n-values prior to cold forming operations to enable planning of acceptable safe deformation with minimal risk of excessive strain hardening and subsequent tear Large angle bends often necessary in building construction (Fig.2) need to be limited to lower boron content. When the composition of the reinforcement bars has been confirmed, the position of the boron levels on the graph in Fig.4 can be used to identify the safe levels of deformation that will not occasion dangerous work hardening.

In view of the fact that hot rolled stock is row material for cold working, knowledge of possible behavior of steel upon cold working given its composition enables the engineer to determine the acceptable level of deformation prior to failure. This can be accomplished from Fig.4.

REFERENCES

[1] Kenichi H, Z., Keiou N. and I Keisuke "Determination of True Stress– Strain Curves of Sheet Metals in Post Uniform Elongation Range" Materials Transactions, Vol. 50, No. 1, pp. 138-144, 2009 .

[2] R. Honeycombe, H. Bhadeshia, Steels: Microstructure and Properties, 3rd Ed. Butterworth Heinemann, Burlington, USA, 2006.

[3] F.H. William. Mechanical Behavior of Materials. 2nd Ed. Cambridge University Press,USA, 2012.

[4] Maalekian M. "The Effects of Alloying Elements on Steels" Christian Doppler Laboratory, 2007.

[5] S.F. Wang, Y. Peng and Z. J. Li "Work-Hardening and Deformation Mechanism of Cold Rolled Low Carbon Steel". Research Journal of Applied Sciences, Engineering and Technology, Vol. 5,No. 3, pp. 823-828, 2013.

[6] Z. Pirowski, J. Wodnicki, J. Olszyński "Micro-additions of Boron and Vanadium in ADI, Part 1. Literature review" Archives of Foundry Engineering, Vol.7, No. 1, pp.167-170, 2007.

[7] H. Caoa, J. Mina, S. Wua, "Pinning of Grain Boundaries by Second Phase Particles in Equal Channel Angularly Pressed Cu–Fe–P Alloy", Elsevier, Materials Science and Engineering. Vol. 7, No.1 167 – 170, 2007.

[8] W. D. Callister, Fundamentals of Materials Science and Engineering; An Integrated Approach: 2ndEdn, John Wiley and Sons, Hoboken, UK, 2005.

[9] S. Seung, B. Min, "Boron Solution and Distribution in Iron α: Application to Boron Steel" The American Physical Society, Vol. 81, No. 14, 2010.

[10] A.K. Chakrabarti, Casting Technology and Cast Alloy, 2nd. Ed., Prentice Hall of India, New Delhi, India 2005.

[11] G. D. Haley "Nitrogen Levels in Ductile Iron" The 2002 Ductile Iron Society Annual Meeting Pioneer Resort and Marina; Oshkosh, Wisconsin, 2012.

[12] M. El-Shennawy, A. I. Farahat, M. I. Masoud and A. I. Abdel-Aziz "Effect of Boron Content on Metallurgical and Mechanical Characteristics of Low Carbon Steel" International Journal of Mechanical Engineering, Vol. 5, Issue 2, pp 2319-2259, 2016.

[13] US 155-2: Steel bars for reinforcement of concrete-Part 2: Ribbed Bars., Uganda Standard.